特约专栏

Phase Diagrams and Thermodynamics of Materials for Energy Applications

Hans Juergen Seifert
(Karlsruhe Institute of Technology, Institute for Applied Materials (IAM-AWP),
Hermann-von-Helmholtz-Platz 1 Eggenstein-Leopoldshafen 76344, Germany)

Abstract: CALPHAD in combination with key experiments has been used to investigate multicomponent multiphase reactions in materials systems relevant for energy engineering. Our results for four different such systems are reviewed. Focus is laid on liquid phase sintering of SiC (LPSSiC), conversion-type Lithium batteries, TiAl-based alloys with chromium additions and zirconia-base thermal barrier coatings, respectively. Typically, findings from CALPHAD-type thermodynamic calculations can be used to define key experiments for further clarification of phase diagrams and thermodynamic properties. The experimental data can then be used vice versa as input for refinement of the CALPHAD models and improved assessment of model parameters. All parameters are adjusted by Thermodynamic Optimization. The datasets are then used to calculate reliable phase diagrams (isothermal sections, isopleths, volatility diagrams) and liquidus surfaces.

Key words: materials for energy; CALPHAD; LPSSiC; Lithium batteries; TiAl-based alloys; thermal barrier coatings
CLC number: TG113 **Document code**: A **Article ID**: 1674 - 3962(2015)04 - 0289 - 08

相图热力学在能源材料中的应用

Hans Juergen Seifert
(卡尔斯鲁厄理工学院 应用材料物理研究所, 德国 埃根施泰因-莱奥波尔茨港 76344)

摘 要: CALPHAD 结合关键实验可以探究能源材料体系的多元多相反应。介绍了 4 个基于不同应用背景的合金体系的评估工作: 液相烧结的 SiC(LPSSiC)体系、转换型锂离子电池体系、掺杂 Cr 的 TiAl 基合金体系以及 Zr 基热障涂层体系。研究结果显示: CALPHAD 热力学计算结果可以用于指导关键实验设计, 从而进一步明确研究体系的相图和热力学性质。获得的实验数据又可以作为精炼 CALPHAD 模型和改进模型参数的输入条件。精炼后的模型参数构成的热力学数据库可用于计算各种相图(包括等温截面、垂直截面、可以用来计算可信的相图(等温截面、垂直截面及波动图)及液相面投影图。

关键词: 能源材料; CALPHAD; LPSSiC; 锂离子电池; TiAl 基合金; 热障涂层

1 Introduction

The development of advanced engineering materials is the key for technical improvements of gas and steam turbine technologies and introduction of new engineering components for power plant applications. Also the efficient use of renewable energies (solar, wind) and energy storage technologies (thermal, electrochemical, chemical) requires the development of completely new engineering materials adjusted to the specific operational facility requirements. For such energy applications thermodynamic calculations are a major fundamental tool for analyzing multicomponent heterogeneous reactions in the relevant metallic alloys and technical ceramics. In this regard the CALPHAD approach (CALculation of PHAse Diagrams) is widely used for clarification of stable and metastable phase equilibria and the coupled thermochemical data[1-2]. The results contribute to the understanding of the microstructure development of engineering materials under environmental conditions dominating during their synthesis and processing as well as commercial use. Looking at phase equilibria as reference state, their knowledge also allows kinetic effects in materials behavior to be evaluated with higher reliability. Computational thermodynamics according to CALPHAD has to provide analytical descriptions of all thermodynamic functions of state of the particular materials system considered. These descriptions are based on models oriented to the (crystal) structures and physico-chemical properties of the phases. Especially the site-occupancies of the crystallographic Wyckoff-positions in solution phases have to be taken into account. Within the so-called Thermodynamic Optimization of the CALPHAD approach, model parameters are adjusted to experimental values which are quantitatively connected to the thermodynamic properties. Of major interest are phase equilibrium data, calorimetric heat measurements, and emf- and vapor pressure data related to chemical potentials. This ap-

Received date: 2014 - 12 - 10
Corresponding author: Hans Juergen Seifert, Professor, Email: Hans. Seifert@ kit. edu
DOI: 10. 7502/j. issn. 1674 - 3962. 2015. 04. 05

proach was, and is, used in our research work for modeling liquid and solid solution phases occurring in engineering materials for energy applications. The thermodynamic model parameters for the systems are assessed based on the available (own and literature) experimental data on phase equilibria and thermodynamic measurements. The results from CALPHAD also provide information about mutual consistency of different types of experimental data and thus the guidelines for further experimental investigations can be defined.

This paper reviews our research work on ceramic and metallic alloy systems of very different characters regarding their engineering materials properties and applications. However, in all cases similar experimental analytical methods as well as CALPHAD-type modeling for phase diagrams and thermodynamic investigations can be used. Four materials classes are selected in this paper: In the first chapter thermodynamic calculations for better understanding of the liquid phase sintering of SiC are presented and compared with experimental results. The following paragraph refers to electrochemical energy storage and describes the possibilities of coupling phase diagrams, thermochemistry and electrochemical behavior for conversion-type Lithium batteries. Subsequently, a metallic alloy system, Ti-Al-Cr, is introduced and it is shown how preliminary calculations can be used to define required key experiments. Based on the results, the information on the homogeneity ranges of the solid solution phases and their phase equilibria can be clarified in detail. Such data can then be used for further refinement of modeling and establishing the thermodynamic datasets. The final chapter describes the strategy for evaluation and assessment of zirconia-based systems for applications in thermal barrier coatings for turbine technologies.

2 Thermodynamic calculations for Liquid Phase Sintered SiC (LPSSiC)

Silicon carbide (SiC) is one of the promising engineering materials for a manifold of power plant applications because of its excellent high-temperature mechanical properties and chemical stability, wear and oxidation resistance[3-4]. It is also interesting for being potentially used as inert matrix fuel material for irradiation of plutonium and minor actinides because of its irradiation damage tolerance[5-8]. In the past decades liquid phase sintered silicon carbide (LPSSiC) has been developed as an engineering construction material with high fracture toughness and other excellent mechanical properties. Alumina, yttria, and aluminum nitride (Al_2O_3, Y_2O_3, AlN) are typically used as sintering additives in LPSSiC and allow a significant reduction of sintering temperatures compared to Solid State Sintered SiC (SSiC). Silicon oxide (SiO_x) (always present on the surface of SiC powder particles) can react with sintering additives e. g. Al_2O_3 and Y_2O_3 (total fraction of about 10 wt% in the initial powder mixture of SiC and additives). In combination with the additives, SiO_x forms an oxide liquid phase at even lower temperatures than the oxide liquid phase produced by reactions between Al_2O_3 and Y_2O_3 alone. The liquid phase partially crystallizes during LPSSiC sample cooling and mostly forms rare earth aluminates and silicates, respectively.

To understand heterogeneous equilibrium phase reactions which can occur during sintering and subsequent thermal treatments of LPSSiC, a thermodynamic dataset for the Si-C-Al-Y-O system was developed for thermodynamic calculations[9-10]. The thermodynamic dataset was established by the CALPHAD method of thermodynamic optimization: analytical descriptions for the Gibbs free energy functions of solid and liquid phases and gaseous species in the Si-C-Al-Y-O system were assessed. As a first step, we analyzed the phase reactions in the Si-C-Y-O subsystem and the thermodynamic compatibilities of Y-silicates ($Y_2Si_2O_7$, Y_2SiO_5) with SiC. Fig. 1 shows a calculated volatility diagram where the condensed phase stabilities are presented at a temperature of 1 650 ℃ as a function of the partial pressures of the major forming gaseous species CO and SiO, respectively. Obviously, the environmental conditions (temperature, partial pressures) during heat treatments have to be fixed very precisely to end up with required phase assemblages. The sublattice model described in the compound energy formalism was used for the treatment of the solid phases. In a refined modeling, the liquid phase was described by using the partially ionic liquid model presented as $(Al^{3+}, Si^{4+}, Y^{3+})_P (O^{2-}, SiO_4^{4-}, Va, AlO_{3/2}, SiO_2, C)_Q$, which covers metallic liquid and oxide liquid as a single phase[10].

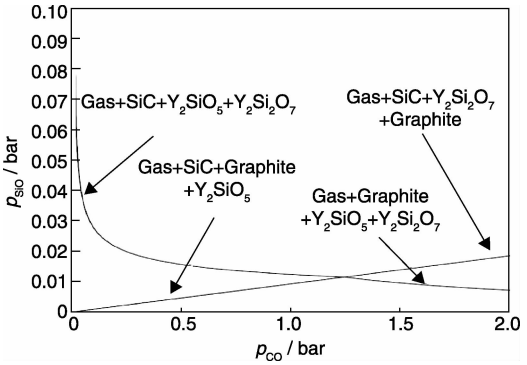

Fig. 1 Volatility diagram at 1 650 ℃ for compatible compositions based on Y_2SiO_5 and $Y_2Si_2O_7$

Obviously another key subsystems in the quinary Si-C-Al-Y-O system is the Y_2O_3-Al_2O_3-SiO_2 system. Fig. 2 shows its calculated liquidus surface providing crucial information for the liquid phase behavior and primary crystallizations in LPSSiC. It has to be emphasized that material compositions in this

subsystem are not only relevant for LPSSiC but also for the joining of SiC-based engineering components using Yttrium aluminosilicate glass solders of chemical composition equivalent to the SiO_2-rich eutectic composition in the system at 1 625 K[11]. In this regard, thermodynamic equilibrium calculations can also contribute to a better understanding of the crystallization behavior of the glasses[12].

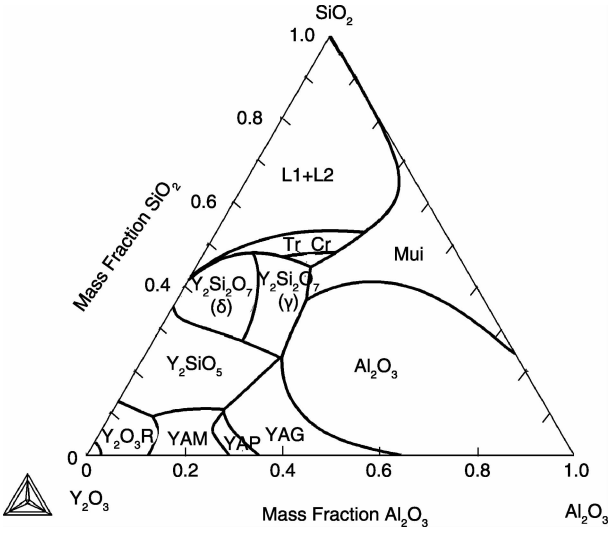

Fig. 2　The calculated liquidus surface of the Al_2O_3-Y_2O_3-SiO_2 system

Using the Si-C-Al-Y-O quinary thermodynamic dataset, the influence of Al_2O_3 and Y_2O_3 as additives in SiC liquid phase sintering was investigated by calculations and compared with experimental data. A simplification was made by not considering of SiC solubility in the liquid phase. Calculated phase fractions of the liquid phase formed for different Al_2O_3/Y_2O_3 ratios and SiO_2 contents at temperature 1 925 ℃ are presented in Fig. 3. Calculations show a slight increase of liquid amount with the increase of SiO_2 content and practically no dependence on the Al_2O_3/Y_2O_3 ratio. We also calculated the sub-solidus phase relations at 1 673 K and compared them to our own experimental results showing reasonable.

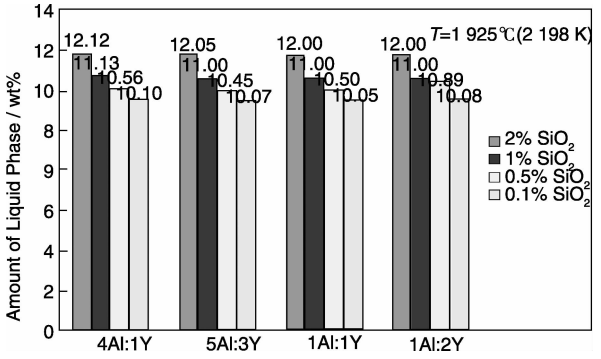

Fig. 3　Calculated amount of liquid phase in a material with 10 wt. % additives depending on the Al_2O_3/Y_2O_3 additive mole ratio at 1 925 ℃ for different SiO_2 contents (amount in wt. %) in the additives

3　Copper oxides as conversion-type electrode materials in Lithium batteries

Copper oxides are of commercial interest to be used as conversion-type electrodes in advanced lithium batteries[13]. The theoretical-specific capacity of e. g. CuO is as high as 674 mAh/g but the material is not yet in major commercial use because of capacity fading during its cycling in electrochemical cells. Much more scientific clarification of materials behavior in battery operation is required to improve the conversion-type battery performance. Thermodynamic calculations can support the better understanding of the fundamental equilibrium materials reaction mechanisms. This is most important as reference information for better evaluation of the kinetic effects and side reactions which are observed during electrochemical cycling. Therefore, a thermodynamic description of the Li-Cu-O system was developed based on literature data as well as on our own experimental determination of the phase stabilities of ternary phases in the Li-Cu-O system[14-15]. Fig. 4 shows the calculated Li-Cu-O isothermal section at 298. 15 K at 1 bar total pressure. Additionally the equilibrium voltages, the activities of oxygen are shown. Thermodynamic descriptions for three ternary phases were taken into account: LiCuO, Li_2CuO_2 and $LiCu_2O_2$, respectively.

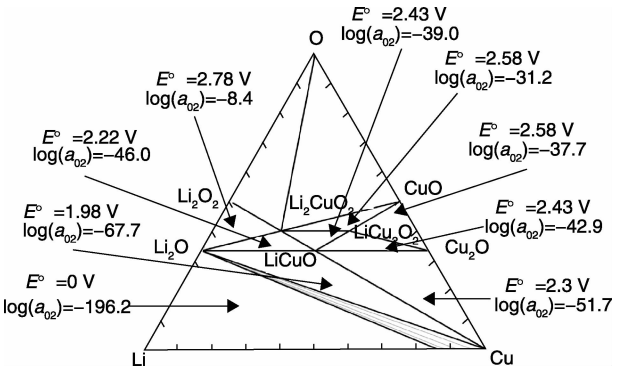

Fig. 4　Calculated Li-Cu-O phase diagram at 298. 15 K. The activities are given relative to the pure element O_2 (gas, 1 bar).

So called titration curves can be calculated along selected composition paths using the Nernst equation. They give the equilibrium cell voltage as a function of lithium content in the cathode compartment of the cell. In addition, the entropy of the cell reaction can be derived from the temperature dependence of the equilibrium voltage. These equilibrium state and the ideal properties show the upper limit of the different parameters. From the Li-Cu-O database, the reactions of CuO and Cu_2O with lithium (electrochemical half cell simulation) were calculated. The reaction of CuO with Li is shown in Fig. 5 and three voltage plateaus are detected. At first, the reaction path goes along the tie line of CuO-$LiCu_2O_2$ showing an

equilibrium voltage of 2.583 V at room temperature. Upon crossing the $LiCu_2O_2$ compound, the equilibrium voltage drops to 2.429 V and the reaction follows the $LiCu_2O_2$-LiCuO tie line. The potential curve shows an instantaneous decrease to 1.975 V when entering the three phase field LiCuO-Li_2O-Cu. In a three phase field, the chemical potential of lithium does not change which results into the potential plateaus. When crossing the two phase field Cu-Li_2O the potential of lithium changes continuously from 1.975 V of the invariant equilibrium involving LiCuO to 0 V at the invariant equilibrium under participation of metallic lithium as shown in the inset in Fig. 5.

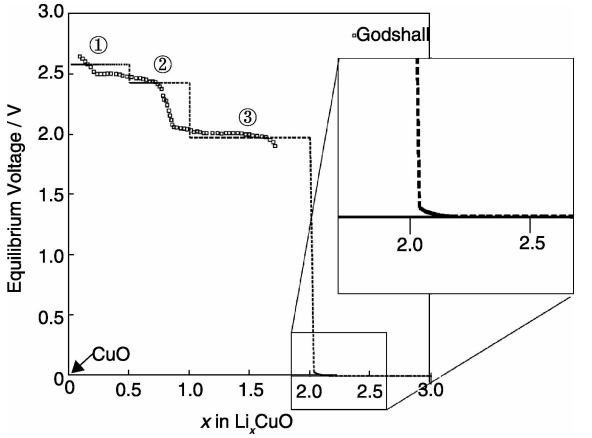

Fig. 5 Calculated titration curve of the reaction of CuO with Li at 298.15 K (dashed line) compared to literature data (open squares)

The temperature dependence of the plateau voltages calculated from the titration curves is shown in Table 1. With increasing temperature, the equilibrium voltages of plateaus 1 and 2 increase, whereas that of plateau 3 decreases. This leads to a positive entropy of reaction for the first two cell reactions, the formation of $LiCu_2O_2$ from CuO and LiCuO from $LiCu_2O_2$. The formation of Li_2O and Cu during the reaction of LiCuO with Li has a negative reaction entropy.

Table 1 Temperature dependence of the plateau voltages calculated from the titration curves

Temperature /K	Plateau 1 /V	Plateau 2 /V	Plateau 3 /V
233.15	2.571	2.410	2.011
273.15	2.578	2.422	1.989
298.15	2.583	2.429	1.975
333.15	2.589	2.439	1.955

4 Ti-Al-Cr alloys for turbine technologies

Titanium aluminides are materials for high-temperature applications e. g. in gas turbines because of their low density, high-temperature strength, and creep and oxidation resistance. Some are already used in commercial aircraft turbines. The ultimate aim of TiAl-based alloy development is construction of powerful and efficient light weight turbines which can save fuel and lower emissions of environmentally toxic gases. Addition of ternary elements to the TiAl-based alloys, such as chromium, can improve their low temperature ductility[16] and oxidation resistance[17]. However, developing of such advanced high temperature engineering Ti-Al materials requires a deep understanding of possible stable and metastable heterogeneous phase reactions which can occur during alloy preparation and under operational conditions. In the course of our research, the phase equilibria in the ternary Ti-Al-Cr system at 1 473 K were experimentally clarified. The experiments were planned on the basis of thermodynamic calculations which were performed earlier in our research group by Cupid et al[18]. Fig. 6 shows a corresponding calculated isothermal section for a temperature of 1473 K in comparison with experimental data from three research groups. Due to the uncertainty in experimental data, the ternary τ-phase was considered stoichiometric by Cupid et al[18].

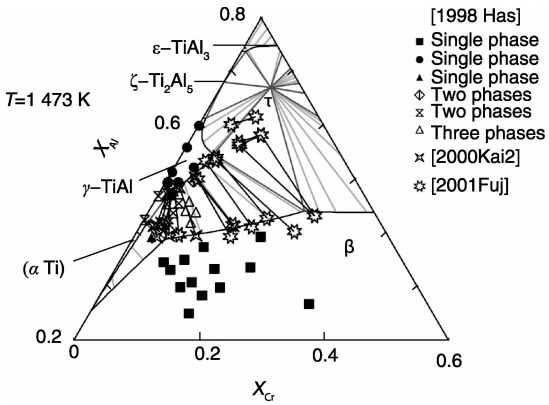

Fig. 6 Calculated partial isothermal sections at 1 473 K by Cupid *et al.*[18] and experimental data

Obviously, it is necessary to clarify experimentally the homogeneity ranges of this τ-phase as well as ternary extensions of binary phases which had to be neglected due to inconsistencies in available experimental literature data. Of specific interest was the clarification of the ternary homogeneity ranges of the β-phase and the C14-Laves phase, respectively. More experiments were required as a base for a refined modeling taking into account crystal structures of the phases and site occupancies of Wyckoff-positions with different species as a function of temperature and composition. Based on the preliminary calculated results by Cupid et al., indicating the major two-phase and three-phase equilibria in the isothermal section at 1 473 K, a total of 18 key alloy compositions could be defined for the further studies. A compositional range of up to 75

at.% Al was considered. The alloys were prepared by arc-melting and subsequent heat treatment and quenching using a vertically arranged tube furnace. The chemical compositions of the quenched samples as well as the chemical compositions of the individual phases in the samples were determined using electron probe microanalysis with wavelength-dispersive X-ray spectroscopy (EPMA/WDS). The phase composition of the samples was obtained using X-ray diffraction (XRD). The spatial distribution of individual phases was obtained from the scanning electron micrographs taken using back-scattered electrons (SEM/BSE) and from electron back-scatter diffraction (EBSD) experiments. Details of the elaborate sample preparation and analyses can be found in the corresponding publication[19].

Based on these results a partial isothermal section was constructed which is in good accordance with the originally calculated section but providing much more detailed information on the homogeneity range of the ternary τ-phase and the ternary extensions of the β-, the γ-, the $(Al_8Cr_5)_h$ and the C14 Laves phases, respectively (Fig. 7). A continuous solid solution of the β-phase at 1 473 K was confirmed which is of major relevance for the preparation of commercial alloys. The next required step in research is the refined thermodynamic modeling of the Ti-Al-Cr system taking into account the data as described here plus our additional experimental results in regard to the liquidus and solidus surfaces[20] and thermodynamic data for intermetallic phases in the system[21].

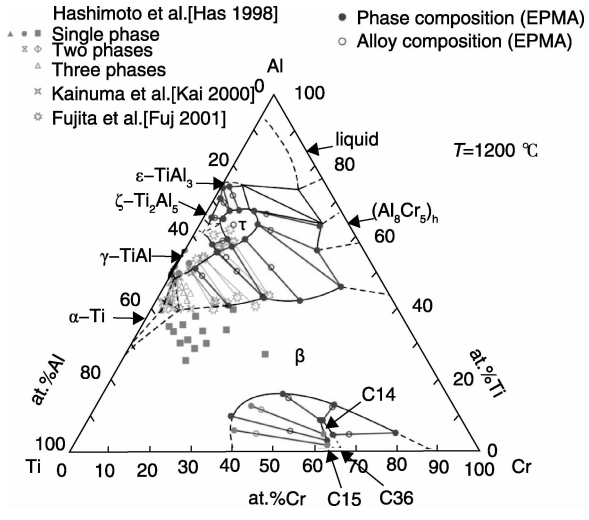

Fig. 7　Phase equilibria in the Ti-Al-Cr system at 1 473 K

5　Zirconia for thermal barrier coatings

The knowledge on phase equilibria and thermodynamics in the ZrO_2-RE_2O_3-Y_2O_3-Al_2O_3 system (RE = Rare Earth elements) including the binary and ternary subsystems is most important for several industrial energy applications. Y_2O_3-stabilised ZrO_2 (YSZ) is commercially used as an engineering material for thermal barrier coatings (TBC) to protect Ni-base superalloys in gas turbine technology, as an electrolyte in solid oxide fuel cells (SOFC) and oxygen sensors, as well as a refractory material for high temperature furnaces and oxidation catalysts. Earlier experimental investigations showed that RE_2O_3 additives decrease the thermal conductivity of YSZ thus making it a promising material for TBC[22].

Therefore, RE_2O_3 co-doped YSZ and $RE_2Zr_2O_7$ (pyrochlore structure for RE = La – Gd) are possible candidates for new TBC materials. Using thermodynamic databases for quaternary ZrO_2-RE_2O_3-Y_2O_3-Al_2O_3 systems (RE = La, Nd, Sm, Gd, Yb) it is possible to evaluate the stability of new candidate materials for TBC and their compatibility with Thermally Grown Oxides (e. g. Al_2O_3 forming as TGO between Ni-base superalloys and TBC during gas turbine operation). Each of the five quaternary systems (with La, Nd, Sm, Gd and Yb, respectively) consists of six binary and four ternary subsystems. Common to all these quaternary systems is the ZrO_2-Y_2O_3-Al_2O_3 system. One major scientific aim of this project was to describe the complex solution phases in the ZrO_2-RE_2O_3-Y_2O_3-Al_2O_3 systems using the sublattice model and the two-sublattice partially ionic liquid model expressed in the compound energy formalism, see e. g. publications[23-25].

Experimental phase diagrams were not available at all for several of the constituent systems such as La_2O_3-Y_2O_3-Al_2O_3, Nd_2O_3-Y_2O_3-Al_2O_3, ZrO_2-Sm_2O_3-Y_2O_3 and Sm_2O_3-Y_2O_3-Al_2O_3. Our strategy followed again was to calculate the phase diagrams of these systems first by extrapolation from binary subsystems. From the results key experiments and analyses to be done can be derived for each system. The experimental studies of ternary systems allow revealing inconsistencies in binary and ternary systems from literature. Thus the project had to combine extended literature data evaluation, own experimental studies, and advanced thermodynamic modelling based on the crystal chemistry of solid solution phases.

This included assessment (Thermodynamic Optimization) of model parameters for binary and ternary oxide systems using computational materials thermodynamics (CALPHAD approach). The results contribute to the understanding of high temperature compatibilities and stabilities of (potentially) commercial materials (for e. g. thermal barrier coatings) in this system. Thermodynamic datasets based on diverse types of

experimental information were developed and phase diagrams calculated and compared with experimental data from our work and literature. The general goals and work tasks in the ZrO_2-RE_2O_3-Y_2O_3-Al_2O_3 systems (RE = La, Nd, Sm, Gd, Yb) were:

(1) Development of thermodynamic model for the pyrochlore solid solution based on crystal structure and site occupancies e. g. $(La^{+3}, Y^{+3}, Zr^{+4})_2(Zr^{+4}, Y^{+3}, La^{+3})_2(O^{-2}, Va)_6(O^{-2})_1(Va, O^{-2})_1$.

(2) The crystal structure based modelling of all other solid solution phases, i. e. (a) fluorite type phases, (b) tetragonal zirconia solid solution phases, (c) C-bixbyite structures, and (d) perovskite solid solution phases and liquid phase.

(3) Thermodynamic description of the available experimental data on homogeneity ranges of solid solutions and phase equilibria in ZrO_2-based systems.

(4) To calculate multicomponent-multiphase heterogeneous phase equilibria and reactions in the ZrO_2-RE_2O_3-Y_2O_3-Al_2O_3 systems.

(5) Experimental verification of calculated results and vice versa using experimental data for refining thermodynamic descriptions.

(6) Development of a self-consistent thermodynamic database for the ZrO_2-RE_2O_3-Y_2O_3-Al_2O_3 systems (RE = La, Nd, Sm, Gd, Yb).

(7) To calculate phase relations relevant to thermal barrier coating stability and interaction with thermally grown oxide based on the developed thermodynamic databases.

The solid solution phases were modeled with the sublattice model expressed in the compound energy formalism. A special challenge was the thermodynamic modeling for pyrochlore phase which had to be based on the crystal structure with five different sites with strong preference of RE^{+3} to the first site, Zr^{+4} to the second site, O^{-2} to the third and fourth sites and vacancies to the fifth site. This description causes the following sublattice modelling: $(RE^{+3}, Zr^{+4})_2(Zr^{+4}, RE^{+3})_2(O^{-2}, Va)_6(O^{-2})_1(Va, O^{-2})_1$. All calculations were made using Thermo-Calc program set (including PARROT and POLY-3 programs). Different types of phase diagrams (isothermal sections, isopleths, potential diagrams) as well as thermodynamic functions, phase fraction diagrams and liquidus surface projections were calculated.

Experimental studies were performed to cross-check the results of thermodynamic modelling and computer simulations and vice versa to refine thermodynamic descriptions. All oxide samples were prepared by the co-precipitation method. The compositions of all samples (before pyrolysis) and filtrates were investigated by Inductively Coupled Plasma Optical Emission Spectrometry (ICP OES). The samples (from heat treatment or thermal analysis) were analyzed by X-ray Diffraction, Scanning Electron Microscopy (SEM / EDX) and Electron Probe Microanalysis (EPMA). High Temperature Differential Thermal Analysis (DTA) was used to investigate phase transformations in the samples. Additionally, Differential Scanning Calorimetry (DSC) was used to measure heat capacities. Rietveld method was applied for crystallographic characterizations.

Some results for the investigations in the ZrO_2-Sm_2O_3-Y_2O_3-Al_2O_3 system are described here. Phase diagrams of two binary systems Sm_2O_3-Y_2O_3 and Sm_2O_3-Al_2O_3 and three ternary systems ZrO_2-Sm_2O_3-Y_2O_3, Sm_2O_3-Y_2O_3-Al_2O_3 and ZrO_2-Sm_2O_3-Al_2O_3 were experimentally studied. The experimental data obtained in this project for the Sm_2O_3-Y_2O_3 system by long term heat treatments and DTA investigation were in agreement with literature data. It was found in our studies that the $Sm_4Al_2O_9$ phase is not stable at temperatures below 1 998 K and these data were used in the assessment of the Sm_2O_3-Al_2O_3 system. The calculated phase diagram is presented in Fig. 8.

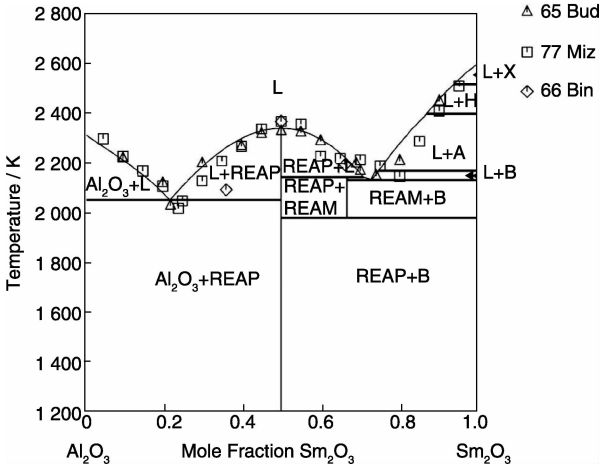

Fig. 8 Calculated phase diagram of the Sm_2O_3-Al_2O_3 system along with experimental data

Comparison of calculations based on binary extrapolations with experimental results indicated inconsistencies for the ZrO_2-Sm_2O_3-Y_2O_3 system. Therefore four compositions of Sm_2O_3-Y_2O_3 system were investigated by high temperature equilibration and DTA. The obtained results indicated good agreement with earlier experimental data and calculations. Therefore ternary interaction parameters were introduced in B, C and fluorite phases, interactions between Sm and Y in fluorite phase and solubility of Y_2O_3 in pyrochlore phase were modelled. The calculated isothermal section at 1 523 K is presented in Fig. 9 along with results of XRD study.

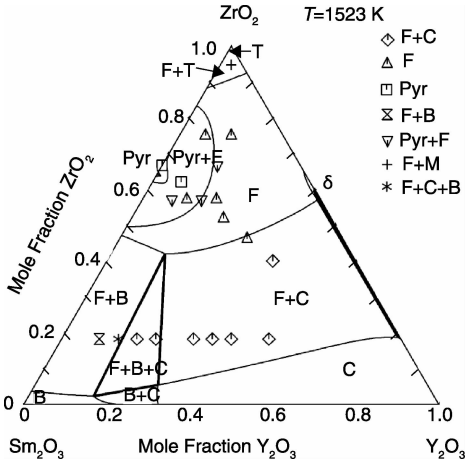

Fig. 9　Isothermal section at 1 523 K for the ZrO_2-Sm_2O_3-Y_2O_3 system in comparison with experimental data

Inconsistencies between calculations and experimental data in the Sm_2O_3-Y_2O_3-Al_2O_3 system in the Sm_2O_3-rich compositions were assumed to be due to the $Sm_4Al_2O_9$ instability in the Sm_2O_3-Al_2O_3 system at temperatures below 1 873 K. Based on a new obtained binary description, the Sm_2O_3-Y_2O_3-Al_2O_3 system and mixing parameter of $(Y, Sm)_4Al_2O_9$ solid solution was optimized to reproduce experimental data on isothermal sections at 1 523, 1 673 and 1 873 K. The calculated isothermal section at 1 523 K is presented in Fig. 10 along with results of XRD study.

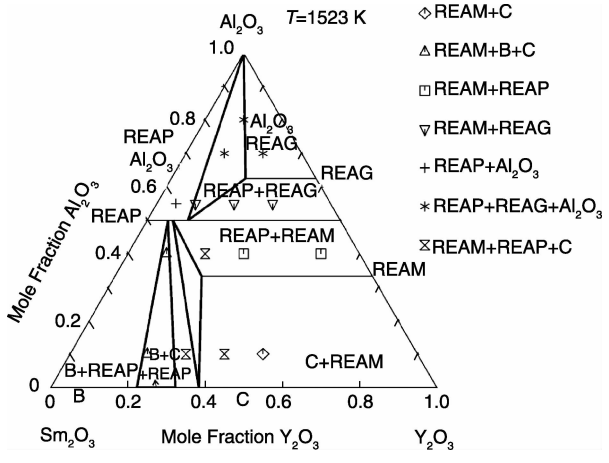

Fig. 10　Isothermal section at 1 523 K for the Sm_2O_3- Y_2O_3- Al_2O_3 system in comparison with experimental data

Also the clarification of melting behavior in the Al_2O_3-rich compositions of Sm_2O_3-Y_2O_3-Al_2O_3 system using DTA and SEM/EDX investigation was undertaken. Obtained results for eutectic reaction were used for optimization of ternary mixing parameter in liquid phase and liquidus surface of the Sm_2O_3-Y_2O_3-Al_2O_3 system was calculated. The new Sm_2O_3-Al_2O_3 thermodynamic description was introduced into database for the ZrO_2-Sm_2O_3-Al_2O_3 system and phase diagrams (isothermal sections, vertical sections) and liquidus surface was re-calculated. The experimental and calculated results obtained in present project are presented in paper[25]. Thermodynamic databases for the ternary systems derived in this project were combined with our previous data for the ZrO_2-Y_2O_3-Al_2O_3 system into the quaternary ZrO_2-Sm_2O_3-Y_2O_3-Al_2O_3 system description.

6　Conclusion

This paper reviews some of our research work using CALPHAD approaches in combination with key experimental studies to clarify phase diagrams and thermodynamics of ceramic and metallic alloys systems. The four system cases selected here refer to engineering materials of major interest in energy applications and cover liquid phase sintering of SiC (LPSSiC), conversion-type Lithium batteries, TiAl-based alloys with chromium additions and zirconia-base thermal barrier coatings, respectively. These are quite different materials systems in regard to their chemical and physical behaviors but can be treated with similar approaches to clarify the underlying phase diagrams and thermochemistry. Preliminary CALPHAD-type thermodynamic calculations are helpful to define key experiments for further research and study. This can relate to the clarification of phase diagrams using e. g. X-ray diffraction (with Rietveld analysis), Electron Microscopy in combination with EDX, Electron Probe Microanalysis (EPMA) and Thermal Analysis (e. g. DTA, TGA, Dilatometry). Also key thermodynamic properties such as enthalpies, heat capacities and entropies (using Calorimetric methods e. g. DSC) can be measured as well as electrochemical data. From such information, the CALPHAD-type modeling and the resulting thermodynamic datasets can be improved and used for supporting application-oriented research and development in energy materials and engineering.

References

[1] Lukas H L, Fries S G, Sundman B. *Computational Thermodynamics: The Calphad Method*[M]. Cambridge: Cambridge University Press, 2007: 324.

[2] Seifert H J, Aldinger F. Applied Phase Studies[J]. *Z Metallkd*, 1996, 87: 841 – 853.

[3] Omori M, Takei H. Pressureless Sintering of SiC[J]. *J Am Ceram Soc*, 1982, 65: 92

[4] Ralf Riedel. *SiC Based Hard Materials*, *Handbook of Ceramic Hard Materials*, *2nd ed*[M]. Weinheim: Wiley-VCH, 2000: 683 – 748.

[5] Krstic V D, Vlajic M D, Verrall R A. Silicon Carbide Ceramics for Nuclear Application[J]. *Key Eng Mater*, 1996, 122-124: 387 – 396

[6] Verrall R A, Vlajic M D, Krstic V D. Silicon Carbide as an Inert-

Matrix for a Thermal Reactor Fuel[J]. *J Nucl Mater*, 1999, 274(2-3): 54-60

[7] Sarma K H, Fourcade J, Lee S G, *et al*. New Processing Methods to Produce Silicon Carbide and Beryllium Oxide Inert Matrix and Enhanced Thermal Conductivity Oxide Fuels [J]. *J Nucl Mater*, 2006, 352(1-3): 324-333

[8] Pan Z, Seifert H J, Fabrichnaya O, *et al*. Phase Reactions of Ceria in LPSSiC, High Temperature Corrosion and Materials Chemistry 7[C]// Wuchina E, Opila E, Fergus J, *et al*. *Proceedings of 214th ECS Meeting*. Honolulu: 2008: 65-80

[9] Cupid D M, Fabrichnaya O, Seifert H J. Thermodynamic Aspects of Liquid Phase Sintering of SiC Using Al_2O_3 and Y_2O_3[J]. *Int J Mater Res*, 2007, 98(10): 976-986.

[10] Pan Z, Fabrichnaya O, Seifert H J, *et al*. Thermodynamic Evaluation of the Si-C-Al-Y-O System for LPS-SiC Application [J]. *J Phase Equilibria and Diffusion*, 2010, 31: 238-249.

[11] Lippmann W, Knorr J, Wolf R, *et al*. Laser Joining of Silicon Carbide- A New Technology for Ultra-high Temperature Resistant Joints [J]. *Nucl Eng Des*, 2004, 231: 151-161.

[12] Ahmad S, Ludwig T, Herrmann M, *et al*. Phase Evaluation During High Temperature Long Heat Treatments in the Y_2O_3-Al_2O_3-SiO_2 System[J]. *J European Ceram Soc*, 2014, 34: 3 835-3 840.

[13] Poizot P, Laruelle S, Grugeon S, *et al*. Nano-Sized Transition-Metaloxides as Negative-Electrode Materials for Lithium-Ion Batteries[J]. *Nature*, 2000, 407: 496-499.

[14] Lepple M, Adam R, Cupid D M, *et al*. Thermodynamic Investigations of Copper Oxides Used as Conversion Type Electrodes in Lithium Ion Batteries[J]. *J Mater Science*, 2013, 48: 5 818-5 826.

[15] Lepple M, Cupid D M, Franke P, *et al*. Heat Capacities of $LiCu_2O_2$ and CuO in the Temperature Range 323 ~ 773 K and Cu_2O in the Temperature Range 973 ~ 1 273 K[J]. *J Phase Equilibria and Diffusion*, 2014, 35: 650-657.

[16] Soboyejo W O, Mercer C. On the Influence of Microstructure on the Fracture Behavior of Gamma-Based Titanium Aluminides. II. Effects of Alloying with Mn[J]. *Mater Manuf Process*, 1996, 11: 431-448.

[17] Lee D B, Kim S H, Niinobe K, *et al*. Effect of Cr on the High Temperature Oxidation of Ll_2-type Al_3Ti Intermetallics[J]. *Mater Sci Eng A*, 2000, 290: 1-5.

[18] Cupid D M, Kriegel M J, Fabrichnaya O, *et al*. Thermodynamic Assessment of the Cr-Ti and First Assessment of the Al-Cr-Ti Systems[J]. *Intermetallics*, 2011, 19: 1 222-1 235.

[19] Kriegel M J, Pavlyuchkov D, Cupid D M, *et al*. Phase Equilibria at 1473 K in the Ternary Al-Cr-Ti System[J]. *J Alloys and Compounds*, 2013, 550: 519-525.

[20] Kriegel M, Pavlyuchkov D, Chmelik D, *et al*. Constitution of the Liquidus and Solidus Surfaces of the Al-Ti-Cr System[J]. *J Alloys and Compounds*, 2014, 584: 438-446.

[21] Kriegel M J, Pavlyuchkov D, Fabrichnaya O, *et al*. Specific Heat Capacity Measurements of Intermetallic Phases in the Ternary Al-Ti-Cr System[J]. *J Phase Equilibria and Diffusion*, 2014, 35: 658-665.

[22] Levi C G. Emerging Materials and Processes for Thermal Barrier Systems[J]. *Curr Opin Solid State Mater Sci*, 2004(8): 77-91.

[23] Fabrichnaya O, Seifert H J. Assessment of Thermodynamic Functions in the ZrO_2-Sm_2O_3-Al_2O_3 System[J]. *J Alloys Comp*, 2009, 475: 86-95.

[24] Fabrichnaya O, Kriegel M J, Seidel J, *et al*. Calorimetric Investigation of the $La_2Zr_2O_7$, $Nd_2Zr_2O_7$, $Sm_2Zr_2O_7$ and $LaYO_3$ Compounds and CALPHAD Assessment of the La_2O_3-Y_2O_3 System [J]. *Thermochimica Acta*, 2011, 526: 50-57.

[25] Fabrichnaya O, Savinykh G, Zienert T, *et al*. Phase Relations in the ZrO_2-Sm_2O_3-Y_2O_3-Al_2O_3 System: Experimental Investigation and Thermodynamic Modeling[J]. *Intern J Mater Res*, 2012, 103: 1 469-1 487.

(编辑 惠 琼)